Hindawi Publishing Corporation
International Journal of Photoenergy
Volume 2016, Article ID 2152018, 9 pages
http://dx.doi.org/10.1155/2016/2152018

Research Article

Numerical Investigations and Analysis of Cu_2ZnSnS_4 Based Solar Cells by SCAPS-1D

M. Djinkwi Wanda,[1,2] S. Ouédraogo,[1,3] F. Tchoffo,[1] F. Zougmoré,[3] and J. M. B. Ndjaka[1,2]

[1] *Université de Yaoundé I, Faculté des Sciences, Département de Physique, BP 812, Yaoundé, Cameroon*
[2] *Centre d'Excellence Africain en Technologies de l'Information et de la Communication (CETIC), Université de Yaoundé I, BP 8390, Yaoundé, Cameroon*
[3] *Laboratoire des Matériaux et Environnement (LA.M.E), UFR-SEA, Université de Ouagadougou, 03 BP 7021, Ouaga 03, Burkina Faso*

Correspondence should be addressed to M. Djinkwi Wanda; martialwanda@gmail.com

Received 1 November 2015; Revised 16 February 2016; Accepted 7 April 2016

Academic Editor: Mahmoud M. El-Nahass

This paper reports numerical investigation, using SCAPS-1D program, of the influence of Cu_2ZnSnS_4 (the so-called CZTS) material features such as thickness, holes, and defects densities on the performances of ZnO:Al/i-ZnO/CdS/CZTS/Mo solar cells structure. We found that the electrical parameters are seriously affected, when the absorber thickness is lower than 600 nm, mainly due to recombination at CZTS/Molybdenum interface that causes the short-circuit current density loss of 3.6 mA/cm^2. An additional source of recombination, inside the absorber layer, affects the short-circuit current density and produces a loss of about 2.1 mA/cm^2 above this range of absorber thickness. The J-V characteristic shows that the performance of the device is also limited by a double diode behavior. This effect is reduced when the absorber layer is skinny. Our investigations showed that, for solar cells having a CZTS absorber layer of thin thickness and high-quality materials (defects density ~10^{15} cm^{-3}), doping less than 10^{16} cm^{-3} is especially beneficial. Such CZTS based solar cell devices could lead to conversion efficiencies higher than 15% and to improvement of about 100 mV on the open-circuit voltage value. Our results are in conformity with experimental reports existing in the literature.

1. Introduction

Nowadays, one of the hottest topics in photovoltaic (PV) field is the study of Cu_2ZnSnS_4 (also known as CZTS) based solar cells. Indeed, thin film of the kesterite compound CZTS is one of the most prospective materials to be used as solar cell absorber layer, due to its excellent optical properties (the band gap varies from 1.4 to 1.5 eV and the absorption coefficient is higher than 10^4 cm^{-1} [1–4]), as well as its constituents that are nontoxic and very abundant naturally. However, despite the development of several physical and chemical fabrication techniques of PV devices [5–9], CZTS based thin films solar cells exhibit relatively weak conversion efficiencies (about 8.4% [9]), compared to those of other technological paths of photovoltaic field, like CIGS based solar cells which reach record efficiencies over 20% [10]. Several reasons could explain this situation, such as various loss mechanisms due to absorber features. Therefore, a detailed analysis of the effect of thickness, holes, and defects densities of CZTS layer is necessary and has been presented in this work, from computations performed using the one dimensional numerical simulation package SCAPS-1D [11]. The results proposed in this study are a useful guideline for design of high performances CZTS based solar cells.

2. Materials and Methods

2.1. Cell Structure. Figure 1 visualizes our solar cell structure, which reads (Ni/Al)MgF_2/ZnO:Al/i-ZnO/CdS/CZTS/Mo/Substrate. As explained in [12], CZTS and CdS, which are, respectively, the absorber and buffer layers, form the p-n junction and constitute the key parts of the device. The intrinsic ZnO (i-ZnO) and ZnO doped with aluminum

Table 1: Baseline parameters for modeling CZTS solar cells [9, 13, 14].

General device properties				
	Front			Back
S_e (cm/s)	10^7			10^5
S_h (cm/s)	10^5			10^7
Layer properties				
	CZTS	CdS	ZnO-I	ZnO:Al
w (nm)	Variable	100	80	450
E_g (eV)	1.45	2.4	3.3	3.3
X (eV)	4.1	4.215	4.4	4.4
$\varepsilon/\varepsilon_0$	7.0	10.0	9.0	9.0
N_c (cm^{-3})	2.2×10^{18}	2.2×10^{18}	2.2×10^{18}	2.2×10^{18}
N_v (cm^{-3})	1.8×10^{19}	9.1×10^{18}	1.8×10^{19}	1.8×10^{19}
ν_e (cm/s)	1×10^7	1×10^7	1×10^7	1×10^7
ν_h (cm/s)	1×10^7	1×10^7	1×10^7	1×10^7
μ_e (cm^2/Vs)	6×10^1	1×10^2	1×10^2	1×10^2
μ_h (cm^2/Vs)	2×10^1	2.5×10^1	2.5×10^1	2.5×10^1
Doping (cm^{-3})	Variable (a)	1×10^{18} (d)	1×10^{18} (d)	1×10^{20} (d)
Bulk defect properties				
N (cm^{-3})	Variable (A)	6×10^{16} (D)	1×10^{16} (D)	1×10^{16} (D)
σ_e (cm^2)	1.3×10^{-12}	1×10^{-12}	1×10^{-15}	1×10^{-15}
σ_h (cm^2)	1.5×10^{-15}	1×10^{-15}	1×10^{-12}	1×10^{-12}
Interface properties				
				CZTS/CdS
ΔE_C (eV)				−0.115
N (cm^{-2})				10^{11} (n)
σ_e (cm^2)				10^{-15}
σ_h (cm^2)				10^{-15}

(a) and (d) denote shallow acceptor and donor defects while (A) and (D) denote deep acceptor and donor defects and (n) denotes neutral defects.

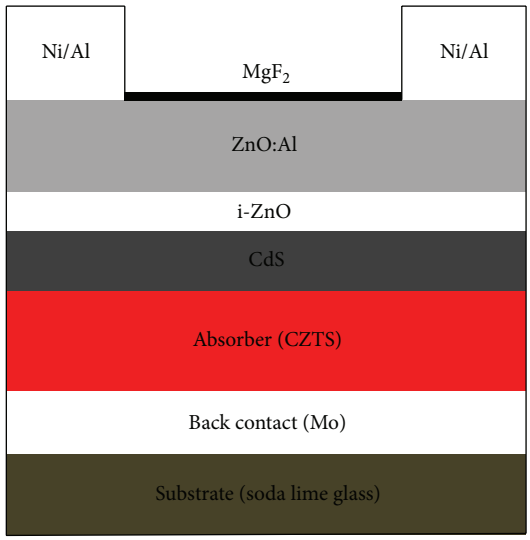

Figure 1: Structure of CZTS based solar cells.

(ZnO:Al) layers are used as transparent conductive oxide and are covered with an antireflection layer (MgF_2).

2.2. Numerical Modeling and Material Parameters. We have used the SCAPS-1D program to simulate the functioning of our solar cell. The baseline parameters used to perform our computations are listed in Table 1. They were borrowed from previous works [9, 13, 14] or obtained by reasonable estimates in some cases. We have introduced one type of single level defects in each layer and the recombinative defect states have been positioned in the narrow distribution close to the middle of band gap such as recommended by Gloeckler et al. [15]. Open-circuit limitation due to interface recombination is a known problem in a wide band gap chalcopyrite solar cell, particularly when the absorber layer conduction band is higher than that of the buffer layer resulting in a "cliff" type band alignment [14]. This is the case of CZTS based solar cells, as shown in the band diagram (Figure 2). To take into account recombination at the CZTS/CdS interface, reasonable neutral interface defects for recombination were also positioned at midgap. As mentioned in [4], the front and back surface reflectivity were set to 0.1 and 0.9, respectively. This high reflectivity at back-contact allows photons crossing the absorber to be reflected in order to optimize the absorption in the absorber. For this purpose, the absorption coefficient has been set to 10^5 cm^{-1} and all SCAPS-1D simulations

Table 2: Simulated results compared to experimental data of [9].

	η (%)	V_{oc} (mV)	J_{sc} (mA/cm^2)	FF (%)
Experimental data	8.4	661	19.5	65.8
Our results without CZTS/CdS interfaces states	8.4	749	19.5	57.48
Our results with CZTS/CdS interfaces states	8.4	748	19.5	57.48

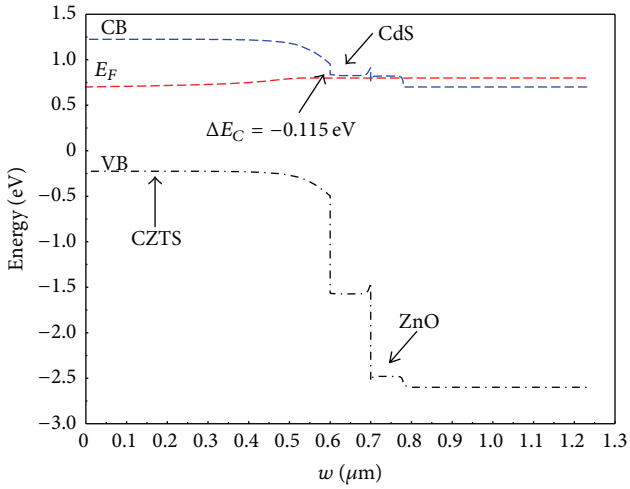

Figure 2: Band diagram obtained from our CZTS solar cell baseline.

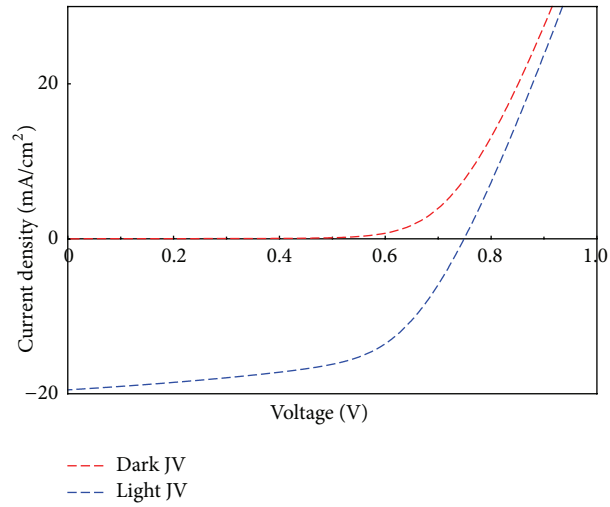

Figure 3: Simulated light and dark current-voltage curves.

were performed under an AM 1.5 light spectrum, while the operating temperature and series resistance have been fixed to 300 K and 4.5 Ω·cm^{-2}, respectively.

Figure 3 shows dark and light J-V curves simulated for our CZTS based solar cell baseline, where the default values of the absorber thickness, the doping, and the defects density are set to 600 nm, 3×10^{15} cm^{-3}, and 1×10^{16} cm^{-3}, respectively. The resulting performance parameters such as efficiency (η), open-circuit voltage (V_{oc}), short-circuit current density (J_{sc}), and fill factor (FF) are obtained using J-V curves.

Our simulated results are presented in Table 2 and compared to experimental data [9].

The short-circuit current density and the efficiency have the same values as those obtained by Shin et al. [9]. The experimental CZTS based solar cell shows a low open-circuit voltage, compared to our value. As stated in [16, 17], this difference can be explained by either the existence of second phase often present at the absorber/back-contact or absorber/buffer layer interface, which increase interface recombination. It can also be due to the greater value of the defects density in the real samples, as predicted in Section 3.3. According to Table 2, there is a good agreement between the experimental data from the literature [9, 14] and our model; therefore, validate our set of parameters as a baseline for simulating the influence of the variation of absorber parameters on the solar cell performance.

3. Results and Discussion

3.1. Effect of the CZTS Layer Thickness on Solar Cell Characteristics. The challenge in thin film solar cells area is to produce solar cells with high conversion efficiency and very thin absorber layer. Works existing in the literature show that the greater efficiencies of CZTS based solar cells have been obtained with thin CZTS layer [9, 14]. In order to obtain qualitative information, we have investigated the effects of the absorber layer thickness on the device electrical parameters. This is shown in Figure 4. The other layers properties are kept constant while varying the absorber thickness. The band gap of the absorber layer is also kept constant to 1.45 eV [9]. We remark that all device performance parameters such as V_{oc}, J_{sc}, and FF are nearly constant for thickness beyond 600 nm, corresponding to the zone where the device presents a relatively weak efficiency.

This is mainly due to high recombination of the photogenerated electrons in the depth of the absorber, which are recombined before reaching the CZTS/CdS interface, because the estimated electron diffusion length is very short in the CZTS absorber (350 nm) [10]. The J_{sc} varies from 21.6 mA/cm^2 (the top value obtained during this simulation) for w = 250 nm to 19.5 mA/cm^2 for w = 600 nm. That is a loss of 2.1 mA/cm^2, which is not negligible, corresponding to recombination current that occurs inside the CZTS based solar cells device with a thicker absorber layer. Figure 5 shows the generation profile made from our baseline. It appears that the generation rate of photogenerated electron-hole pairs is low for a thick CZTS absorber layer because of a relatively high recombination in the bulk material.

In the zone of thin thicknesses, we have selected two domains:

(i) For 250 nm < w < 600 nm, the electrical parameters such as V_{oc}, J_{sc}, and efficiency increase. J_{sc} reaches its

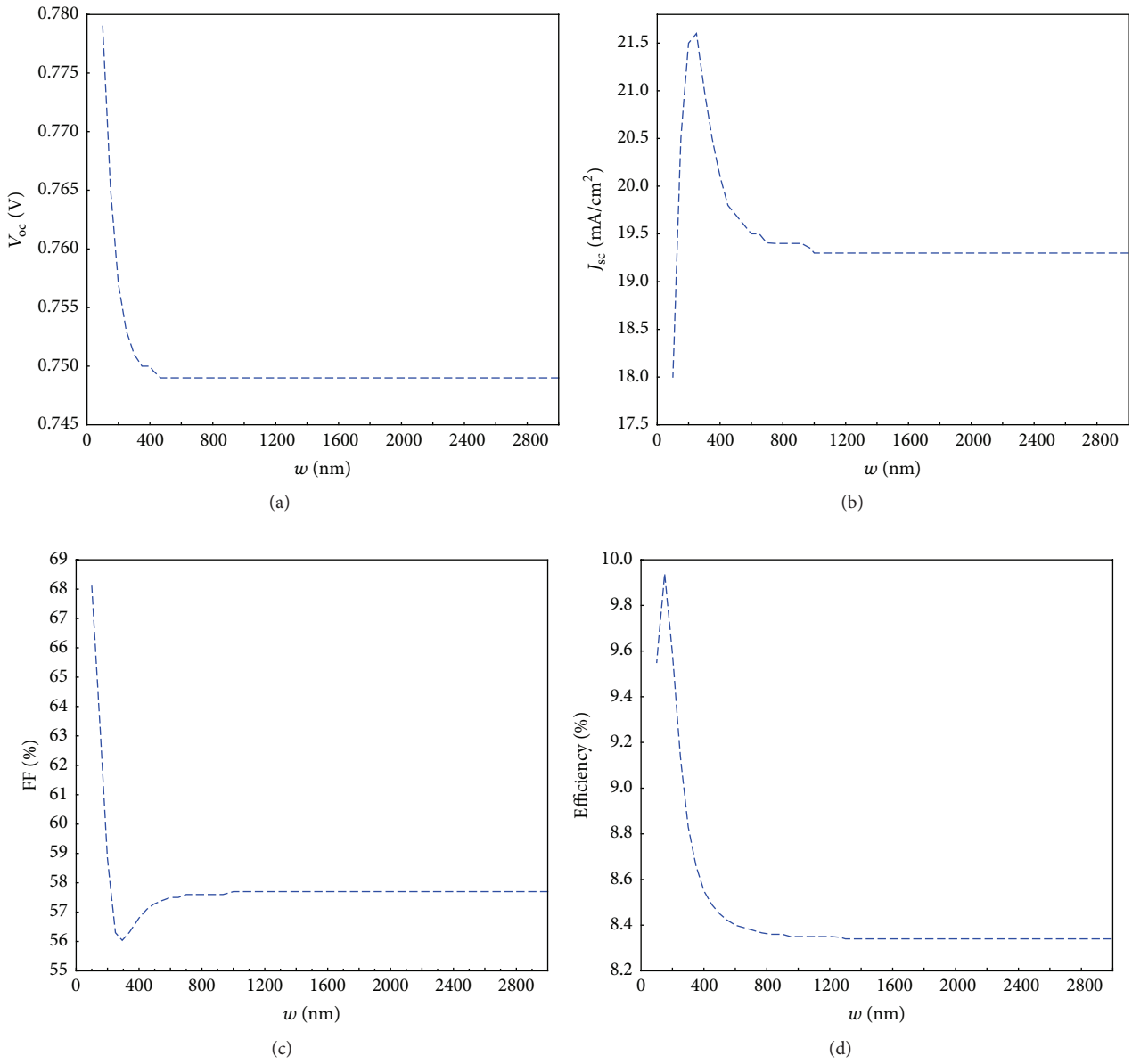

FIGURE 4: Absorber thickness effects on open-circuit voltage (V_{oc}), short-circuit density (J_{sc}), fill factor (FF), and efficiency.

top value for a thickness of 250 nm. This is mainly due to a good collection of carriers across the entire absorber layer thickness. The quantum efficiency curves for different values of absorber thickness are shown in Figure 6. Since the photons of short wavelengths (300 nm $< \lambda <$ 450 nm) correspond to the absorption in the window ZnO and buffer CdS layers, we have chosen to focus solely on those which are effectively absorbed in the CZTS absorber layer (450 nm $< \lambda <$ 900 nm). The quantum efficiency of cells is higher when the thickness decreases and reaches about 84% for w = 250 nm. Therefore, most photons are absorbed for absorber thickness between 250 nm and 600 nm, which increases the solar cell performance.

(ii) For 100 nm $< w <$ 250 nm, V_{oc} and FF increase. The increase of V_{oc} shows the nondegradation of the junction in the case of ultrathin thickness. In the same condition, the increase of FF indicates the minimization of double diode behavior, observed through the nonsuperposition between the dark and light J-V characteristics (Figure 3), which reduces the additional recombination occurring in the p-n junction. J_{sc} decreases rapidly due to the higher recombination of photogenerated electrons close to the back-contact and proves the existence of potential barrier at the CZTS/Molybdenum interface, leading to the removal of the holes to the crossing of this interface. The J_{sc} passes from 21.6 mA/cm^2 for w = 250 nm to 18.5 mA/cm^2 for w = 100 nm, that is, a loss

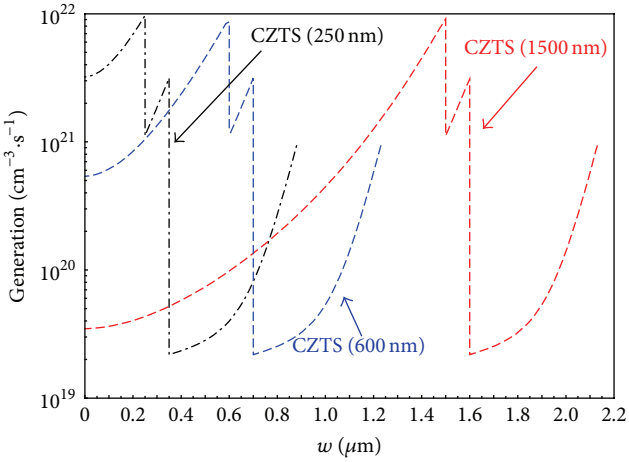

FIGURE 5: Generation profile obtained from our CZTS solar cell baseline.

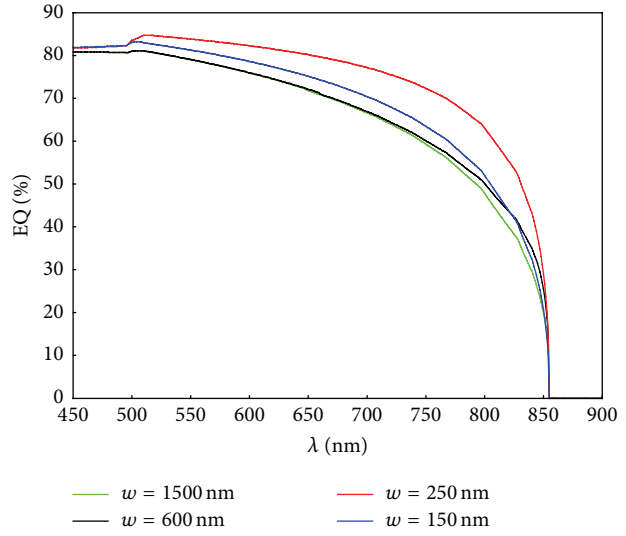

FIGURE 6: Quantum efficiency curves for different values of absorber thickness.

of 3.6 mA/cm^2 corresponding to the recombination current at the back-contact.

In short, we predict that the optimization of the absorber's thickness in CZTS based solar cells is important to improve its performance. For a good collection of the photogenerated electron-hole pairs, the absorber layer thickness may be chosen below 600 nm. These observations are similar to those of [9, 14].

3.2. Effect of Absorber Holes Density. Figure 7 illustrates the influence of the holes density (p) on V_{oc}, J_{sc}, FF, and efficiency for different absorber layer thickness. It shows that V_{oc} increases significantly with the increase of absorber doping, while J_{sc} decreases, both in the same way, whatever the absorber layer thickness is. The increase of V_{oc} becomes fast and important for doping beyond $p = 10^{16}$ cm^{-3}. However, J_{sc} decreases very quickly for doping varying from 10^{16} to 10^{18} cm^{-3} and becomes almost constant above this range. These phenomena can be explained by Shockley equation in the case of simple p-n junction model:

$$V_{oc} = \frac{KT}{q} \ln\left(\frac{J_{Ph}}{J_0} + 1\right). \quad (1)$$

Here, K, T, and q denote the Boltzmann constant, the operating temperature, and the elementary charge, while J_{Ph} and J_0 are, respectively, the photogenerated current density and the saturation current density. The saturation current density is expressed by

$$J_0 = An_i^2 \left(\frac{D_e}{L_n N_A} + \frac{D_h}{L_h N_D}\right). \quad (2)$$

n_i is the intrinsic carriers concentration; D_e and D_h are the electrons and holes diffusion coefficient, respectively; L_e and L_h are the electrons and holes diffusion length, respectively; N_A and N_D are, respectively, the ionized-acceptor atoms and ionized-donor atoms densities; A is the diode quality factor. Since, in the classical p-type semiconductor, we have $p \approx N_A$ in thermodynamic equilibrium, we have made the approximation that the density of acceptors is equal to holes density in the bulk of absorber. Hence, the saturation current density will reduce when p rises. Therefore, V_{oc} increases (Figure 7(a)). The evolution of J_{sc} as a function of the absorber holes density presents three zones, such as illustrated in Figure 7(b), which influence strongly this electrical parameter: the first zone is 10^{12} cm^{-3} $< p <$ 10^{16} cm^{-3}, the second one corresponds to 10^{16} cm^{-3} $< p <$ 10^{18} cm^{-3}, and the third one is p greater than 10^{18} cm^{-3}. In spite of a slight lowering in the first zone, we observe that the short-circuit current density is larger than 18 mA/cm^2 for the thicker absorber layer and maintains itself up to 20 mA/cm^2 for the thinner thicknesses. This improvement of J_{sc} is due to a better collection of the photogenerated electrons, which enhances the efficiency. The efficiency reaches 10.1% for a 150 nm absorber thickness for weakly doped sample. This is mainly due to the fact that the increase of doping, for the thinner thicknesses, reduces the space charge region width (SCRW) and the absorber thickness may become order of magnitude or smaller than the SCRW.

This requirement will be beneficial and crucial when designing the absorber layer thickness of CZTS based solar cells. The reason is that the minority carriers in CZTS materials have a short life time [14]. In the second zone, J_{sc} decreases significantly with the increase of absorber doping, because of the fact that this rising enhanced recombination process of photogenerated electrons and reduced the possibility to collect them. On the other hand, the photogenerated electrons undergo Coulomb interactions because of the overpopulation of doping. This leads to more holes' traps and recombination. Hence, CZTS absorber doping strongly produces more effects which are harmful to device performance parameters (Figures 7(b) and 7(d)). The short-circuit current density, although it is constant, is very low for $p > 10^{18}$ cm^{-3}, whatever the doping is. This is due to various recombination additional mechanisms created

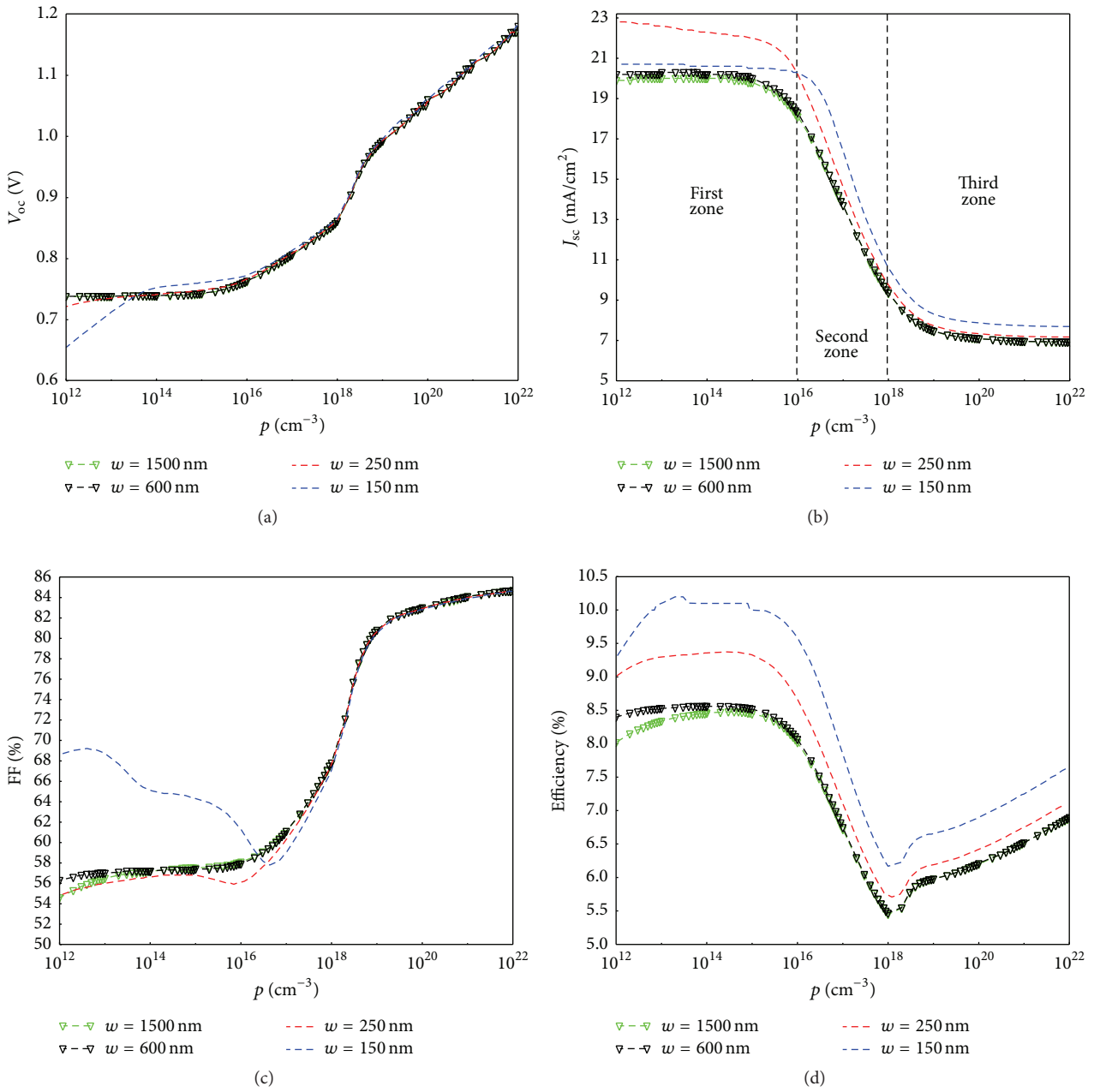

Figure 7: The simulated performance of holes density on V_{oc}, J_{sc}, FF, and efficiency as a function of the CZTS absorber thickness.

by capture centers of photogenerated electrons through the absorber layer which are occasioned by an inhomogeneous distribution of doping in the bulk material. The relative enhancement of efficiency in this range is mainly due to V_{oc} and FF which are affected positively by the rising of doping.

3.3. Effect of Absorber Defects Density. Chen et al. [18] have studied the defect properties of CZTS using first-principle calculations. Their study has shown that the formation energy acceptor defects were lower than donor ones. This reason influences our choice to introduce only single acceptor (−/0) like defects state in the CZTS absorber layer. Figure 8 presents the defects density effects on the solar cell performance parameters. We see that the solar cell performance does not change when the defects density is below 10^{14} cm^{-3}. Once the defects density exceeds this value, the electrical performance parameters are strongly affected although there is a slight increase of FF when it reaches 10^{17} cm^{-3}. The use of a bad quality of CZTS material results in the multiplication of carriers' traps and drives to produce weak efficiency solar cells. Besides, Wang et al. [16] have shown that the activation energy of CZTS absorber is lower than its band gap (1.45 eV). Hence, close to deep defect levels, the increase of defect density also contributes to recombination loss

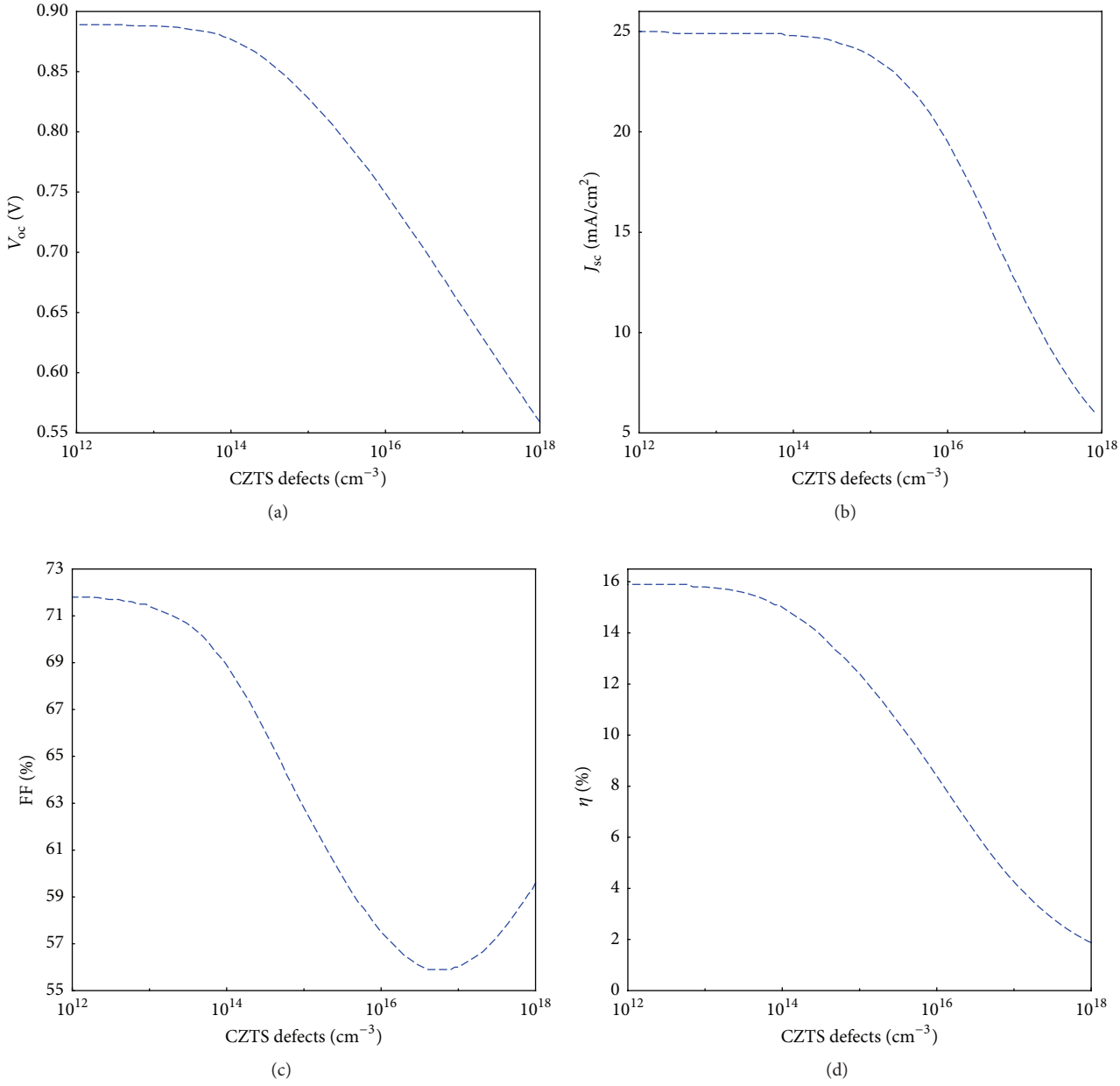

Figure 8: The simulation of defect density effects on the CZTS solar cell performance parameters.

mechanism commonly ascribed to dominant recombination at the buffer/absorber interface. Associated with other recombinations mentioned above, these could explain the stronger loss undergone by the electrical parameters for the defects density up to 10^{16} cm^{-3}. The V_{oc} curve (Figure 8(a)) shows that a source of open-circuit voltage loss in the CZTS based thin film solar cells device also would be the strong concentration of defects that, beyond a density of 3.10^{16} cm^{-3}, brought down V_{oc} under 700 mV. Figure 8(d) shows that the development of CZTS absorber materials with a high quality (defects density ~10^{15} cm^{-3}) is very beneficial for the CZTS based solar cells devices. We predict conversion efficiencies over 15%.

4. Conclusion

Using SCAP-1D package, we analyzed the variations of absorber layer thickness, absorber holes, and defects densities on CZTS based solar cells. We have shown the following facts:

(i) The electrical parameters are affected significantly by increase of absorber thickness. This produces a loss of about 2.1 mA/cm^2 on short-circuit current density due to the recombination inside the absorber layer. Besides, the effect of the double diode phenomenon is much reduced when thickness is thinner and leads to minimization of additional recombination at the p-n junction that causes an important loss of fill

factor. We predict that, for a development of the CZTS based solar cells with high conversion efficiency, the absorber layer thickness must be chosen below 600 nm, because of the short electrons diffusion length in the CZTS compounds. The recombination current density at the back-contact estimated at 3.6 mA/cm^2 shows that a strong potential barrier exists at CZTS/Molybdenum interface.

(ii) The open-circuit voltage and the fill factor are affected positively by the increase of holes density. A doping less than 10^{16} cm^{-3} is beneficial for the CZTS based solar cells and especially for the absorber thickness lower than 600 nm. Above this range of doping, the increase of the population of holes creates supplementary centers of recombination of the photogenerated carriers.

(iii) The performance parameters are seriously affected by the defects. The development of high-quality CZTS materials can allow achievement of the devices having conversion efficiencies up to 15% and could also improve about 100 mV of open-circuit voltage value.

Nomenclature

Abbreviations

AM 1.5:	Air Mass 1.5
CB:	Conductor band
CZTS:	Cu_2ZnSnS_4
SCAPS-1D:	Solar cell capacitance simulator in 1 dimension
SCRW:	Space charge region width
VB:	Valence band.

Symbols

$\varepsilon/\varepsilon_0$:	Dielectric constant
E_g:	Band gap energy of semiconductor
E_F:	Fermi level
FF:	Fill factor
J_{sc}:	Short-circuit current density
μ_e, μ_h:	Electron and hole mobility
N_c, N_v:	States effective densities in the conductor and valence band
N:	Defects density
p:	Holes density
V_{oc}:	Open-circuit voltage
σ_e, σ_h:	Electron and hole capture cross section
S_e, S_h:	Electron and hole surface recombination velocity
ν_e, ν_h:	Electron and hole thermal velocity
X:	Electron affinity
λ:	Wave length
w:	Absorber layer thickness
W:	Layers width.

Competing Interests

The authors declare that they have no competing interests.

Acknowledgments

All simulations reported in this paper have been made with SCAPS-1D program. So, the authors acknowledge Marc Burgelman and his colleagues who have developed this program.

References

[1] A. Wangperawong, J. S. King, S. M. Herron, B. P. Tran, K. Pangan-Okimoto, and S. F. Bent, "Aqueous bath process for deposition of Cu_2ZnSnS_4 photovoltaic absorbers," *Thin Solid Films*, vol. 519, no. 8, pp. 2488–2492, 2011.

[2] H. Araki, Y. Kubo, K. Jimbo et al., "Preparation of Cu_2ZnSnS_4 thin films by sulfurization of co-electroplated Cu-Zn-Sn precursors," *Physica Status Solidi*, vol. 6, no. 5, pp. 1266–1268, 2009.

[3] H. Katagiri, K. Saitoh, T. Washio, H. Shinohara, T. Kurumadani, and S. Miyajima, "Development of thin film solar cell based on Cu_2ZnSnS_4 thin films," *Solar Energy Materials and Solar Cells*, vol. 65, no. 1–4, pp. 141–148, 2001.

[4] W. Zhao, W. Zhou, and X. Miao, "Numerical simulation of CZTS thin film solar cell," in *Proceedings of the 7th IEEE International Conference on Nano/Micro Engineered and Molecular Systems (NEMS '12)*, pp. 502–505, Kyoto, Japan, March 2012.

[5] H. Katagiri, K. Jimbo, S. Yamada et al., "Enhanced conversion efficiencies of Cu_2ZnSnS_4-based thin film solar cells by using preferential etching technique," *Applied Physics Express*, vol. 1, no. 4, Article ID 0412011, 2008.

[6] S. Ahmed, K. B. Reuter, O. Gunawan, L. Guo, L. T. Romankiw, and H. Deligianni, "A high efficiency electrodeposited Cu_2ZnSnS_4 solar cell," *Advanced Energy Materials*, vol. 2, no. 2, pp. 253–259, 2012.

[7] K. Maeda, K. Tanaka, Y. Fukui, and H. Uchiki, "Influence of H_2S concentration on the properties of Cu_2ZnSnS_4 thin films and solar cells prepared by sol–gel sulfurization," *Solar Energy Materials and Solar Cells*, vol. 95, no. 10, pp. 2855–2860, 2011.

[8] A. V. Moholkar, S. S. Shinde, A. R. Babar et al., "Synthesis and characterization of Cu_2ZnSnS_4 thin films grown by PLD: solar cells," *Journal of Alloys and Compounds*, vol. 509, no. 27, pp. 7439–7446, 2011.

[9] B. Shin, O. Gunawan, Y. Zhu, N. A. Bojarczuk, S. J. Chey, and S. Guha, "Thin film solar cell with 8.4% power conversion efficiency using an earth-abundant Cu_2ZnSnS_4 absorber," *Progress in Photovoltaics: Research and Applications*, vol. 21, no. 1, pp. 72–76, 2013.

[10] P. Jackson, D. Hariskos, E. Lotter et al., "New world record efficiency for Cu(In,Ga)Se_2 thin-film solar cells beyond 20%," *Progress in Photovoltaics: Research and Applications*, vol. 19, no. 7, pp. 894–897, 2011.

[11] S. Degrave, M. Burgelman, and P. Nollet, "Modeling of polycrystalline thin cells: news features in scaps version 2.3," in *Proceedings of the 3rd World Conference on Photovoltaic Energy Conversion*, pp. 487–490, Osaka, Japan, May 2003.

[12] S. Ouédraogo, R. Sam, F. Ouédraogo, M. B. Kebre, J. M. Ndjaka, and F. Zougmoré, "Optimization of Copper Indium Gallium Di-Selenide (CIGS) based solar cells by back grading," *Journal of Ovonic Research*, vol. 9, no. 4, pp. 95–103, 2013.

[13] J.-S. Seol, S.-Y. Lee, J.-C. Lee, H.-D. Nam, and K.-H. Kim, "Electrical and optical properties of Cu_2ZnSnS_4 thin films prepared by RF magnetron sputtering process," *Solar Energy Materials and Solar Cells*, vol. 75, no. 1-2, pp. 155–162, 2003.

[14] K. Wang, O. Gunawan, T. Todorov et al., "Thermally evaporated Cu_2ZnSnS_4 solar cells," *Applied Physics Letters*, vol. 97, no. 14, Article ID 143508, 2010.

[15] M. Gloeckler, A. L. Fahrenbruch, and J. R. Sites, "Numerical modeling of CIGS and CdTe solar cells: setting the baseline," in *Proceedings of the 3rd World Conference on Photovoltaic Energy Conversion*, pp. 491–494, May 2003.

[16] K. Wang, B. Shin, K. B. Reuter, T. Todorov, D. B. Mitzi, and S. Guha, "Structural and elemental characterization of high efficiency Cu_2ZnSnS_4 solar cells," *Applied Physics Letters*, vol. 98, Article ID 051912, 2011.

[17] M. Gloeckler and J. R. Sites, "Band-gap grading in $Cu(In,Ga)Se_2$ solar cells," *Thin Solid Films*, vol. 241, pp. 480–481, 2005.

[18] S. Chen, J.-H. Yang, X. G. Gong, A. Walsh, and S.-H. Wei, "Intrinsic point defects and complexes in the quaternary kesterite semiconductor Cu_2ZnSnS_4," *Physical Review B*, vol. 81, no. 24, Article ID 245204, 2010.